

# UAL/ETEAPOT Proton EDM Benchmark Comparisons II: Transfer Matrices and Twiss Functions

J. D. Talman and R. M. Talman

August 30, 2012

## Abstract

UAL/ETEAPOT is used to obtain transfer matrices between arbitrary lattice positions, and, from them, Twiss functions as functions of longitudinal coordinate  $s$ . The same three benchmark lattices as in the April 27, 2012, report “UAL/ETEAPOT Results (Augmented) for Proton EDM Benchmark Lattices” are analysed. The lattices have field indices  $m = -1$ ,  $m \approx 0$ , and  $m = 1$ . For the earlier report once-around transfer matrices had been obtained and used to determine beta functions at the origin and fractional tunes. But general transfer matrices had not been obtained and aliasing ambiguities prevented the determination of integer tune values. Results are compared to values obtained from a linearized transfer matrix formalism. In all cases the design vertical tunes have been adjusted to  $Q_y=0.2$ .

# 1 Parameters of Benchmark Lattices

Table 1: Parameters of benchmark all-electric EDM lattices, and Twiss parameters calculated from linearized transfer matrices.

file name	variable name	unit	E_BM_M1.0.sxf	E_BM_Z.sxf	E_BM_P1.0.sxf
cells/arc	NCellPerArc		20	20	20
bend radius	r0	m	40.0	40.0	40.0
half drift length	Ldh	m	1.0	1.0	1.0
half bend per cell	Thetah	r	0.078539816	0.078539816	0.078539816
half bend length	Leh	m	3.141592	3.141592	3.141592
circumference	circum	m	331.327	331.327	331.327
inverse focal length	q	1/m	-0.002019	-0.00005960	0.0019075
field index	m		-1.0	1.0e-10	1.0
horizontal beta	betax	m	35.9237	36.1018	36.1910
vertical beta	betay	m	264.182	263.620	262.237
horizontal tune	Qx		1.4605	1.4578	1.4588
vertical tune	Qy		0.20024	0.20004	0.20047

## 2 Determination of Twiss Functions From Transfer Matrices

### 2.1 Analysis of the Once-Around Transfer Matrix at the Origin

In this section  $x$  and  $y$  and  $ct$  subscripts will be suppressed, and only transverse evolution is to be discussed. The most general transfer matrix is a six-by-six matrix  $\mathbf{M}(s_i, s_j)$ , which propagates a phase space vector  $\mathbf{x}(s_i)$  at  $s_i$ , to its value  $\mathbf{x}(s_j)$  at  $s_j$ :

$$\mathbf{x}(s_j) = \mathbf{M}(s_i, s_j) \mathbf{x}(s_i). \quad (1)$$

UAL/ETEAPOT starts by assigning coordinates at the origin,  $s_0 = 0$ , to the particles in a standard bunch (as described earlier), and then evolves the standard bunch and records the coordinates  $\mathbf{x}(s_i)$  at all points  $s_i$ . From these results the transfer matrices  $\mathbf{M}(0, s_i)$  can be calculated (also as described earlier). By definition

$$\mathbf{M}(0, 0) = \mathbf{I}, \quad (2)$$

where  $\mathbf{I}$  is the  $6 \times 6$  identity matrix.

To extract Twiss lattice functions one needs “once-around” transfer matrices defined by

$$\widetilde{\mathbf{M}}(s_i) \equiv \mathbf{M}(s_i, s_i + \mathcal{C}_0) = \mathbf{M}(0, s_i) \mathbf{M}(s_i, \mathcal{C}_0). \quad (3)$$

where  $\mathcal{C}_0$  is the circumference of the design orbit; the final step has been taken because knowledge of  $s_i + \mathcal{C}_0$  requires tracking for more than one complete turn, but we are assuming that tracking has been done only for exactly one complete turn. Propagation from  $s = \mathcal{C}_0$  to  $\mathcal{C}_0 + s_i$  is the same as propagation from  $s = 0$  to  $s_i$ . The Twiss parameterization of (one partitioned diagonal  $2 \times 2$  block of) such a once-around, symplectic transfer matrix is

$$\widetilde{\mathbf{M}}(s_i) = \begin{pmatrix} \cos \mu + \alpha \sin \mu & \beta \sin \mu \\ -\frac{1+\alpha^2}{\beta} \sin \mu & \cos \mu - \alpha \sin \mu \end{pmatrix}. \quad (4)$$

Extraction of the  $\alpha_0$  and  $\beta_0$ , the Twiss parameters at the origin, can start from

$$\cos \mu = \frac{1}{2} (\widetilde{\mathbf{M}}_{11}(0) + \widetilde{\mathbf{M}}_{22}(0)), \quad (5)$$

which fixes  $\cos \mu$ . Because of sign ambiguity, this determines only  $|\sin \mu|$ . One also has the relations

$$\beta_0 = \left| \frac{\widetilde{\mathbf{M}}_{12}(0)}{\sin \mu} \right|. \quad (6)$$

and

$$\alpha_0 = \frac{1}{2 \sin \mu} (\widetilde{\mathbf{M}}_{11}(0) - \widetilde{\mathbf{M}}_{22}(0)). \quad (7)$$

With  $\beta$  being positive by convention, from the 1,2 element,  $\text{sign}(\sin \mu)$  can be seen to be the same as  $\text{sign}(\widetilde{\mathbf{M}}_{12})$ . With  $\cos \mu$  known, this fixes  $\sin \mu$ . Together, these relations fix  $\sin \mu$ ,  $\cos \mu$ ,  $\alpha_0$ , and  $\beta_0$ .

Conventionally one also introduces the third Twiss parameter

$$\gamma_0 = \frac{1 + \alpha_0^2}{\beta_0}, \quad (8)$$

which can be obtained once  $\beta_0$  and  $\alpha_0$  have been determined.

Because of the multiple-valued nature of inverse trig functions, these relations do not determine a unique value for  $\mu$ . They do, however, determine the quadrant in phase space in which the angle  $\mu$  resides. For  $\text{sign}(\sin \mu) > 0$  the angle  $\mu$  resides in the first or second quadrant, in which case the fractional tune is less than  $1/2$ ; otherwise the fractional tune is greater than  $1/2$ . For  $\text{sign}(\cos \mu) > 0$  the angle  $\mu$  resides in the first or fourth quadrant, in which case the fractional tune is below  $1/4$  or above  $3/4$ . These considerations fix the fractional parts of the tunes.

An “aliasing” or “integer-tune” ambiguity remains, however, which cannot, even in principle, be obtained from the once-around matrix. Only if both transverse tunes are less than 1 (which is hardly ever the case) would the tunes be equal to the fractional tunes that have been determined. In general, to obtain the integer tunes, it is necessary to analyse the turn by turn data at sufficiently closely-space intermediate points in the lattice.

## 2.2 Evolving the Twiss Functions Around the Ring

To find the Twiss parameters at an arbitrary location  $s_i$  in the ring requires the once-around transfer matrix  $\widetilde{\mathbf{M}}(s_i)$ . This can be obtained most compactly by multiplying the equation

$$\mathbf{M}(0, s_j) = \mathbf{M}(s_i, s_j) \mathbf{M}(0, s_i) \quad (9)$$

on the right by  $\mathbf{M}^{-1}(0, s_i)$  to produce

$$\mathbf{M}(s_i, s_j) = \mathbf{M}(0, s_j) \mathbf{M}^{-1}(0, s_i). \quad (10)$$

Substituting this with  $s_j = \mathcal{C}_0$  into Eq. (3) produces

$$\widetilde{\mathbf{M}}(s_i) = \mathbf{M}(0, s_i) \widetilde{\mathbf{M}}(0) \mathbf{M}^{-1}(0, s_i). \quad (11)$$

Having obtained  $\widetilde{\mathbf{M}}(s_i)$ , the procedure described in the previous subsection can then be used to obtain  $\alpha(s_i)$  and  $\beta(s_i)$ . But the integer tune ambiguity can, again, not be resolved. To resolve this ambiguity both  $x$  and  $y$  phases have to be tracked continuously through the lattice, requiring that they advance continuously and monotonically. (Later, at least in principle, the same ambiguity will have to be faced for longitudinal motion. But the integer longitudinal tune is almost always zero, so the problem will not appear in the longitudinal case.)

UAL/ETEAPOT requires the lattice description to be in the form of an `.sxf` file. To be “legal” the granularity of such a file has to be fine enough that no phase can advance by more than a quarter integer through any element in the file. Before working out the  $\alpha$  and  $\beta$  function evolution, ETEAPOT first works out the total phase advances from the origin to every node specified by the `.sxf` file (or, if some elements are sliced more finely, by every node after slicing).

There is an alternative way of finding the betatron phase advances. It starts with a Twiss parameterization of  $\mathbf{M}(0, s)$  from the origin to an arbitrary position  $s$  in the lattice;

$$\mathbf{M}(0, s) = \begin{pmatrix} \sqrt{\frac{\beta(s)}{\beta_0}} \left( \cos \psi(s) + \alpha_0 \sin \psi(s) \right) & \sqrt{\beta_0 \beta(s)} \sin \psi(s) \\ \sqrt{\frac{\beta_0}{\beta(s)}} \left( \cos \psi(s) - \alpha(s) \sin \psi(s) \right) & \end{pmatrix}. \quad (12)$$

The 2,1 element is quite complicated; it is not shown here since it will not be needed for the following analysis. Dividing the 1,1 element by the 1,2 element produces

$$\frac{\mathbf{M}_{1,1}(0, s)}{\mathbf{M}_{1,2}(0, s)} = \frac{\sqrt{\frac{\beta(s)}{\beta_0}} \left( \cos \psi(s) + \alpha_0 \sin \psi(s) \right)}{\sqrt{\beta_0 \beta(s)} \sin \psi(s)} = \frac{\cot \psi(s) + \alpha_0}{\beta_0}. \quad (13)$$

Rearranging this equation produces

$$\psi(s) = \tan^{-1} \frac{\mathbf{M}_{1,2}(0, s)}{\beta_0 \mathbf{M}_{1,1}(0, s) - \alpha_0 \mathbf{M}_{1,2}(0, s)}. \quad (14)$$

Like all inverse trigonometric formulas, this equation has multiple solutions. But, with the `.sxf` granularity being required to be fine enough, one can (in principle) sequentially obtain unique phases. With  $\psi(s)$  starting from  $\psi(0) = 0$ , as  $s$  increases from  $s_i$  to  $s_{i+1}$  there is a unique solution of Eq. (14),  $\psi(s_i) > \psi(s_{i-1})$  such that the function  $\psi(s)$  increases monotonically, as required. Because the interval from  $s_{i-1}$  to  $s_i$  is non-zero,  $\psi$  will, superficially, advance discontinuously; the correct solution is the least discontinuous. The same calculation has to be done for both the  $x$  and  $y$  betatron sectors. Unfortunately, even though, theoretically, the phase advances monotonically, numerical errors can cause Eq. (14) to give local phase decrease. This can cause Eq. (14) to give occasionally erratic results.

### 2.3 Beta Function Comparisons

Figures 1 and 2 compare  $\beta_x$  evaluations for the “benchmark” lattice `E_BM_Z_sl4.sxf` which has field index  $m = 0$ . This is the lattice closest to “cylindrical” with lumped quadrupoles just barely strong enough to move the lattice away from the boundary between vertical stability and vertical instability. The figure on the left is evaluated by ETEAPOT, the one on the right by the linearized (Wollnik) formulas re-derived in an appendix to the report [3]. There is agreement to excellent accuracy on local beta function dependence  $\beta_x(s)$ . Similarly good agreement for vertical beta function  $\beta_y(s)$  is exhibited in Figures 3 and 4;

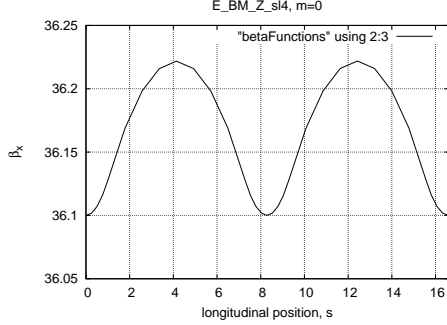


Figure 1:  $\beta_x(s)$  calculated by ETEAPOT for lattice “E\_BM\_Z\_sl4”.

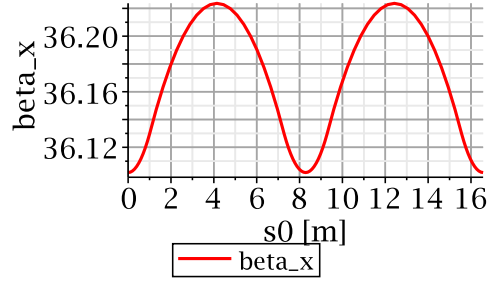


Figure 2:  $\beta_x(s)$  calculated by linearized theory for lattice “E\_BM\_Z\_sl4”.

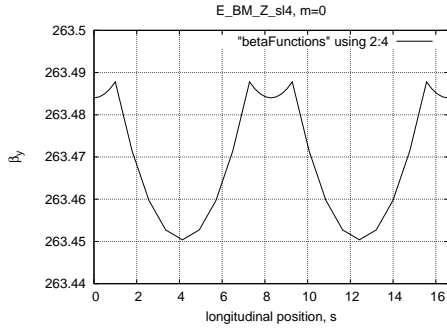


Figure 3:  $\beta_y(s)$  calculated by ETEAPOT for lattice “E\_BM\_Z\_sl4”.

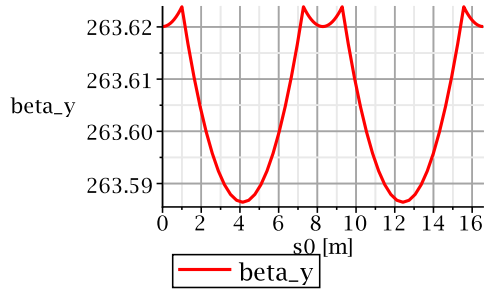


Figure 4:  $\beta_y(s)$  calculated by linearized theory for lattice “E\_BM\_Z\_sl4”.

Figures 5 through 8 contain evaluations for the “benchmark” lattice `E_BM_M1.0_sl4.sxf`. which has field index  $m = -1$ ; in this case the radial electric field  $E_r$  is independent of radial displacement  $x \approx r - r_0$ . Agreement is again excellent.

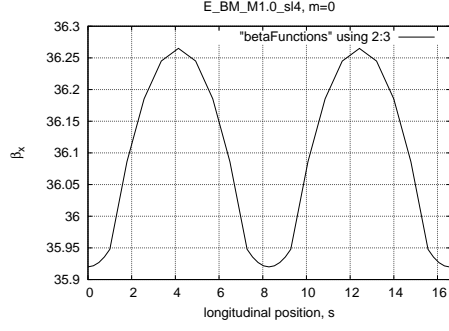


Figure 5:  $\beta_x$  calculated by ETEAPOT for lattice “E\_BM\_M1.0\_sl4”.

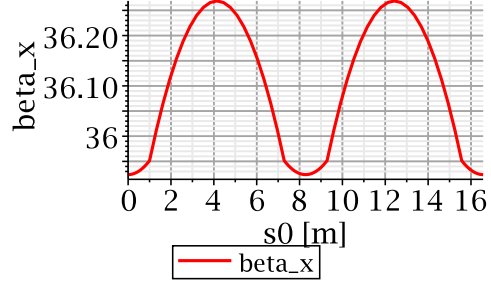


Figure 6:  $\beta_x$  calculated by linearized theory for lattice “E\_BM\_M1.0\_sl4”.

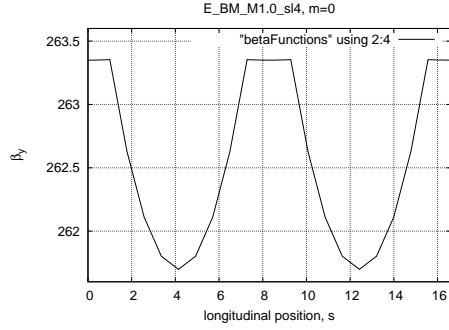


Figure 7:  $\beta_y$  calculated by ETEAPOT for lattice “E\_BM\_M1.0\_sl4”.

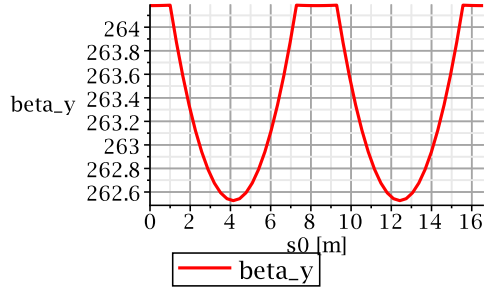


Figure 8:  $\beta_y$  calculated by linearized theory for lattice “E\_BM\_M1.0\_sl4”.

Figures 9 through 12 contain evaluations for the “benchmark” lattice `E_BM_P1.0_sl4.sxf`, which has field index  $m = 1$ ; this is the “Kepler” or “spherical” case with  $E_r \sim 1/r^2$ . Agreement is again excellent.

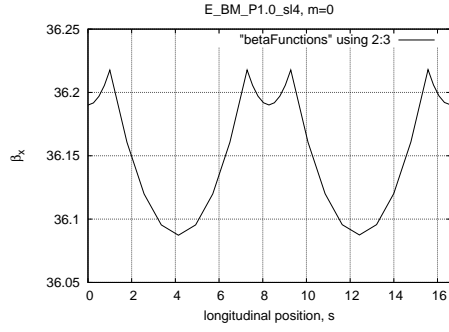


Figure 9:  $\beta_y$  calculated by ETEAPOT for lattice “E\_BM\_P1.0\_sl4”.

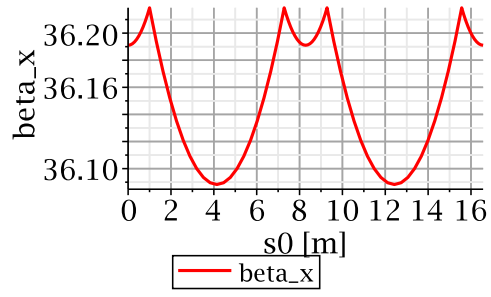


Figure 10:  $\beta_y$  calculated by linearized theory for lattice “E\_BM\_P1.0\_sl4”.

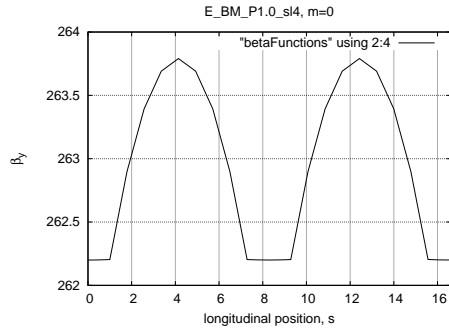


Figure 11:  $\beta_y$  calculated by ETEAPOT for lattice “E\_BM\_P1.0\_sl4”.

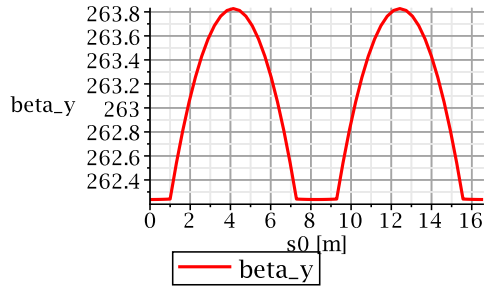


Figure 12:  $\beta_y$  calculated by linearized theory for lattice “E\_BM\_P1.0\_sl4”.

The following tables give parameter values for the same three benchmark lattices.

Table 2: E\_TEAPOT comparisons for E\_BM\_P1.0.sxf.

file name	variable name	unit	linearized	2 slices/bend	
cells/arc	NCellPerArc		20		
bend radius	r0	m	40.0		
half drift length	Ldh	m	1.0		
half bend per cell	Thetah	r	0.078539816		
half bend length	Leh	m	3.141592		
circumference	circum	m	331.327		
inverse focal length	q	1/m	0.0019075		
field index	m		1.0		
horizontal beta	betax	m	36.1910	36.1910	
vertical beta	betay	m	262.237	262.2370	
horizontal tune	Qx		1.4588	1.4588	
vertical tune	Qy		0.20047	0.2005	

Table 3: E\_TEAPOTComparisons for E\_BM\_Z.sxf.

file name	variable name	unit	linearized	2 slices/bend	
cells/arc	NCellPerArc		20		
bend radius	r0	m	40.0		
half drift length	Ldh	m	1.0		
half bend per cell	Thetah	r	0.078539816		
half bend length	Leh	m	3.141592		
circumference	circum	m	331.327		
inverse focal length	q	1/m	-0.00005960		
field index	m		1.0e-10		
horizontal beta	betax	m	36.1018	36.0795	
vertical beta	betay	m	263.620	261.4688	
horizontal tune	Qx		1.4578	1.4581	
vertical tune	Qy		0.20004	0.2018	



Table 4: E\_TEAPOT comparisons for E\_BM\_M1.0.sxf

file name	variable name	unit	linearized	2 slices/bend	
cells/arc	<b>NCellPerArc</b>		20		
bend radius	<b>r0</b>	m	40.0		
half drift length	<b>Ldh</b>	m	1.0		
half bend per cell	<b>Thetah</b>	r	0.078539816		
half bend length	<b>Leh</b>	m	3.141592		
circumference	<b>circum</b>	m	331.327		
inverse focal length	<b>q</b>	1/m	-0.002019		
field index	<b>m</b>		-1.0		
horizontal beta	<b>betax</b>	m	35.9237	35.8566	
vertical beta	<b>betay</b>	m	264.182	251.8522	
horizontal tune	<b>Qx</b>		1.4605	1.4620	
vertical tune	<b>Qy</b>		0.20024	0.2102	

## References

- [1] J.D. Talman and R.M. Talman, *UAL/ETEAPOT Results (Augmented) for Proton EDM Benchmark Lattices*, BNL internal report, April 29, 2012
- [2] N. Malitsky, J. Talman, and R. Talman, *Appendix UALcode: Development of the UAL/ETEAPOT Code for the Proton EDM Experiment*, UAL/ETEAPOT documentation (frequently revised), August, 2012
- [3] Storage Ring EDM Collaboration, *A Proposal to Measure the Proton Electric Dipole Moment with  $10^{-29}$  e-cm Sensitivity*, especially Appendix 1. October, 2011
- [4] C. Møller, *The Theory of Relativity*, Clarendon Press, Oxford, 1952,
- [5] G. Muñoz and I. Pavic, *A Hamilton-like vector for the special-relativistic Coulomb problem*, Eur. J. Phys. **27**, 1007-1018, 2006
- [6] R. Talman, *Geometric Mechanics*, John Wiley and Sons, 2000
- [7] J. Aguirregabiria et al., Archiv:physics/0407049v1 [physics.ed-ph] 2004,
- [8] U. Torkelsson, Eur. J. Phys., **19**, 459, 1998,
- [9] T. Boyer, Am. J. Phys. **72** (8) 992, 2004

### 3 Preview of FNAL Lattice Optics

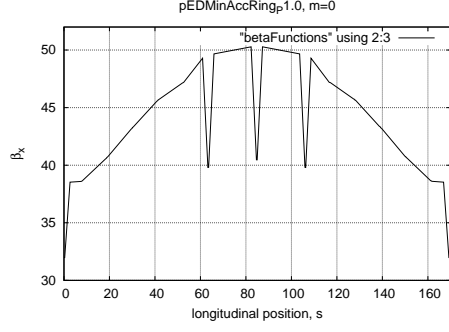


Figure 13:  $\beta_x(s)$  calculated by ETEAPOT for lattice “pEDMinAccRingP1.0”.

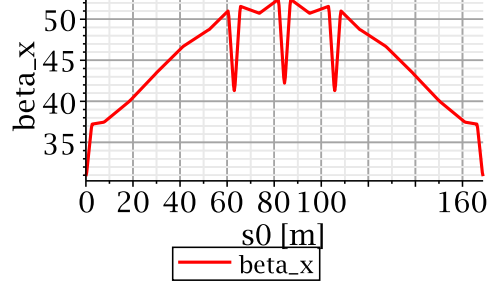


Figure 14:  $\beta_x(s)$  calculated by linearized theory for lattice “pEDMinAccRingP1.0”.

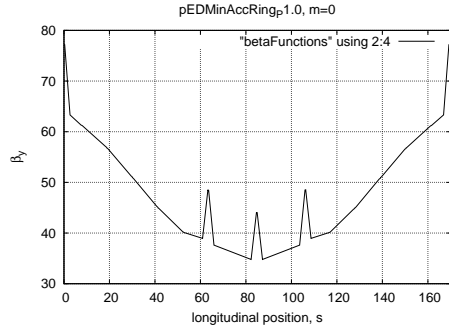


Figure 15:  $\beta_y(s)$  calculated by ETEAPOT for lattice “pEDMinAccRingP1.0”.

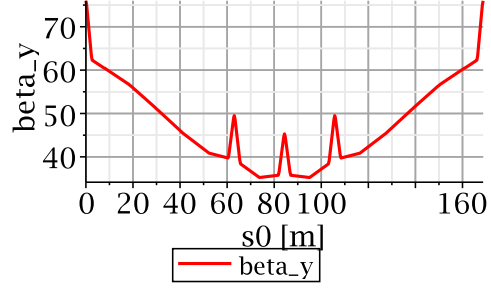


Figure 16:  $\beta_y(s)$  calculated by linearized theory for lattice “pEDMinAccRingP1.0”.